

Background Magnetic Field and Kink and Torus Instabilities

Y. Liu¹

ABSTRACT

Using a Potential Field Source Surface model (PFSS), we study profile of magnetic field overlying erupted filaments. The filaments studied here were reported to experience a kink instability or a torus instability. The kink instability leads to a full eruption or a failed eruption, while the torus instability leads to a full eruption. We found that, in high altitude (from 1.4 Rs to 2.5 Rs. Rs denotes solar radius), the field declines with height more slowly for the full eruption of kink instability than that for the torus instability eruption, which is agreeable with previous numerical MHD simulations. But for failed eruption filaments, the field profiles are steeper than that for the full eruptions. This is inconsistent with the MHD simulations. In low altitude (from 1.1 Rs to 1.3 Rs), they all appear to be comparable. The field strength at low altitude ($\sim 10^5$ km) is much stronger for failed eruption than that for the full eruptions. This implies that the field strength at low altitude is another factor to decide whether or not a full eruption can take place.

Subject headings: Sun: solar eruption—Sun: instabilities—Sun: magnetic field structure

1. Introduction

Kink and torus instabilities are suggested to be two mechanisms for triggering solar flares and Coronal Mass Ejections (CMEs) (Sakurai 1976; Török & Kliem 2005; Kliem & Török 2006). Recent MHD simulations have shown that the gradient of magnetic field overlying the erupted flux ropes decides which instability actually takes place (Kliem & Török 2006; Fan & Gibson 2007), and whether or not a kink instability can eventually develop a successful eruption (Török & Kliem 2005). With MHD simulation, Török & Kliem (2005) modeled a failed eruption of a flux rope led by kink instability. When modified the overlying field to decrease with height more quickly, they found this eruption developed to become a full

¹W. W. Hansen Experimental Physics Laboratory, Stanford University, Stanford, CA94305-4085

eruption. They thus concluded that “the decrease of the overlying field with height is a main factor in deciding whether the instability leads to a confined event or a CME.” The simulation carried out by Fan & Gibson (2007) shows that, for a kink instability eruption, the overlying arcade field declines with height much more slowly than that for a torus instability eruption. They suggest that slow decrease of overlying arcade field with height helps confine the flux rope so that the rope can accumulate sufficient self-helicity for developing a kink instability. If we put these simulations together, we would expect to see a slow decrease of overlying field with height for a confined event of kink instability (or failed eruption. We denotes this kind of events as *FE* hereafter). The gradient of the overlying field becomes steep for a full eruption of kink instability (We denotes this kind of eruptions as *KI* hereafter), and even steeper for a full eruption of torus instability (We denotes this kind of eruptions as *TI* hereafter). In this letter, we investigate magnetic field above the erupted filaments in order to examine whether or not these three types of eruptions can be distinguished observationally, as shown in these MHD numerical simulations. A sample of events that includes the three types of eruptions, namely *TI*, *KI* and *FE*, is collected from literature.

The paper is organized as follow. In Section 2, we describe the events and calculation. The results are presented in Section 3. Finally, we conclude this research in Section 4.

2. Events and analysis

The events we choose for this research are two *TI* events from Schrijver et al. (2007), four *KI* events from Williams et al. (2005) and Green et al. (2007), and four *FE* events from Green et al. (2007). For the two *TI* cases in Schrijver et al. (2007), numerical simulation of a torus instability shows a result better agreeing with observations than other possible models, implying that these two cases are likely to be torus-instability eruptions. All the events in Williams et al. (2005) and Green et al. (2007) exhibit a clearly helical shape when erupted, suggesting a kink instability eruption. The events in Green et al. (2007) also have the same sign between the magnetic helicity of the erupted filaments (twist of magnetic tubes) and the rotation of the filaments, a proxy of writhing of the magnetic tubes. This is strong evidence suggesting development of a kink instability. Among these eight kink instability eruptions, four of them experienced a failed eruption.

The overlying magnetic field was computed from the observed magnetic field over the Sun’s surface based on a Potential Field Source Surface model (PFSS) (Schatten et al. 1969; Altschuler & Newkirk 1969; Hoeksema et al. 1982; Wang and Sheeley 1992). In this model, it is assumed that the magnetic field is potential everywhere between the photosphere and a spherical source surface. The modeled field matches the radial component on the photosphere

and is forced to become purely radial on the source surface. The magnetic field data at solar surface were taken by SOHO/MDI (Scherrer et al. 1995). At each height, the magnetic field strength is averaged over an area of the active regions where the eruptions take place. In this way, the profile of magnetic field as a function of height can be obtained.

To quantitatively compare the field profiles of those events, following Török & Kliem (2007), we also compute the decaying index of the external field, n , assuming $B_{ex} \propto R^{-n}$, where R is height. Figure 1 shows an example of how to calculate the decaying index. Basically, we divide the data into two parts, the low altitude from 1.1 Rs to 1.3 Rs and the high altitude from 1.4 Rs to 2.5 Rs, because the indexes in these two domains appear to be significantly different (see the curves in the left panel of Figure 2). Here Rs represents solar radius. The strength and height are in logarithm. Thus, the decaying index is the slope of a linear fitting to the data, as shown in the Figure.

Listed in Table 1 are a summary of these events. The first column is the type of eruptions. *TI*, *KI* and *FE* represent torus instability eruption, kink instability eruption and failed eruption, respectively. The second and third columns denote flare class and occurrence time. The fourth column is the active region number, followed by the computed decaying indexes in different altitudes. n_1 is the decaying index derived using the high latitude data from 1.4 Rs to 2.5 Rs. n_2 is the index from the low altitude data from 1.1 Rs to 1.3 Rs. The average field strength at 1.1 Rs is in the seventh column. *S*, *G* and *W* in the last column denote the events from Schrijver et al. (2007), Green et al. (2007), and Williams et al. (2005), respectively.

3. Results

Plotted in Figure 2 are magnetic strength as a function of height. The green, red and black curves represent the magnetic profiles for *FE*, *KI* and *TI* events, respectively. The curves in the left panel show the profiles from 1.1 Rs to 2.5 Rs, while in the right panel are the profiles in low altitude from 1.01 Rs to 1.30 Rs. The magnetic field is in logarithm. For comparison, we shift the curves in y-axis so that they all have the same maximum value. From this Figure we can obtain two results. First, in high latitude, the field declines with height more slowly for *KI* (the red curves in the left panel) than that for *TI* (the black curves in the left panel), as shown in the MHD numerical simulation (Fan & Gibson 2007). But in the low altitude, the field profiles look pretty much similar for both types of eruptions. The plot in the right panel even seems to show that the field decreases with height slightly quicker for *KI* than that for *TI*. This is inconsistent with the MHD simulation. It suggests that the field structure in high altitude is more important to decide which instability will

take place. Second, the field profile for *FE* does not look like what MHD simulation suggests, i.e., the field decreases with height more slowly than that for *KI* and *TI*. Instead, the field drops even faster in the high altitude, while it looks similar to *TI* and *KI* in the low altitude.

To make a more quantitative comparison, we average the parameters for each type of eruption (see Table 2). We also put *KI* and *TI* together as a type of full eruption (the bottom row in Table 2) in order to compare with the type of failed eruption (*FE*). Basically, *KI* and *TI* have very similar decaying indexes (n_2) and magnetic strengths (B) in low altitude, but have significantly different decaying indexes in high altitude (n_1). n_1 of *KI* is much smaller than that of *TI*. This is in agreement with MHD simulation. For a comparison of full eruption (*KI+TI*) and failed eruption (*FE*), we can see that *FE* has a greater decaying index (n_1) than *KI+TI* in high altitude, while a comparable index in low altitude. This is inconsistent with MHD simulation. The most outstanding difference between *FE* and *KI+TI* is perhaps the field strength (B) at 1.1 Rs: for failed eruption (27.1 ± 8.5), it is three times of full eruption (9.5 ± 2.9). This may be the main factor to decide whether a full eruption or a failed eruption eventually takes place. In a detailed analysis of a failed eruption of a filament, Ji et al. (2003) reported that the erupted filament reached a maximum height of 8×10^4 km before fell back to the Sun. Schrijver et al. (2007) observed, for the two cases they studied, the onset of the so-called rapid-acceleration phase when the filaments reach a height of $\sim 10^5$ km. This implies that, beside the field gradient as suggested by MHD simulations, the field strength in low altitude ($\sim 10^5$ km) is another factor to decide whether or not a full eruption will occur.

4. Conclusions

In this research, we have studied profiles of overlying magnetic field for ten erupted events, in order to observationally examine the distinguishable characteristic of field profiles for the three types of eruptions, *TI*, *KI* and *FE*, as shown in numerical simulations. It is shown that the field decreases with height more slowly for *KI* than that for *TI*. This agrees with MHD simulations. But it is true only in high altitude (1.4Rs to 2.5Rs). In low altitude, they look pretty much similar. It implies that the field in high altitude alone can also decide which instability occurs.

The field profile of *FE* is much steeper than that of *KI*, which is inconsistent with MHD simulations. The magnetic strength at a height of $\sim 7.0 \times 10^4$ km is much stronger for *FE*, about three times of *KI* or *TI*. It suggests that the field strength in low altitude ($\sim 10^5$ km) is another factor to decide whether or not a full eruption will take place.

The authors thank X. Zhao at Stanford University for providing the PFSS code. This work was supported by the NASA NAG5-13261, and NSF/CISM project under grant ATM-0120950. SOHO is a project of international cooperation between ESA and NASA.

REFERENCES

- Altschuler, M. D., Newkirk, G., Jr. 1969, *Sol. Phys.*, 9, 131
- Fan, Y., Gibson, S. E., 2007, *ApJ*, 668, 1232
- Green, L.M., Kliem, B., Török, T., van Driel-Gesztelyi, L., Attrill, G.D.R., 2007, *Sol. Phys.*, in press.
- Hoeksema, J. T., Wilcox, J. M., Scherrer, P. H. 1982, *J. Geophys. Res.*, 87, 10331
- Ji, H., Wang, H., Schmahl, E. J., Moon, Y.-J., Jiang, Y. 2003, *ApJ*, 595, L135
- Kliem, B., Török, T., 2006, *Phys. Rev. Lett.*, 96, 255002
- Sakurai, T., 1976, *PASJ*, 28, 177
- Schatten, K. H., Wilcox, J. M., Ness, N. F. 1969, *Sol. Phys.*, 6, 442
- Scherrer, P. H., Bogart, R. S., Bush, R. I. et al. 1995, *Sol. Phys.*, 162, 129
- Schrijver, C. J., Elmore, C., Kliem, B., Török, T., Title, A. M., 2007, *ApJ*, in press.
- Török, T., Kliem, B., 2005, *ApJ*, 630, L97
- Török, T., Kliem, B., 2007, *Astronomische Nachrichten*, 328, 743
- Wang, Y. -M., Sheeley, N. R., Jr. 1992, *ApJ*, 392, 310
- Williams, D. R., Török, T., Demoulin, P., van Driel-Gesztelyi, L., Kliem, B. 2005, *ApJ*, 628, L163

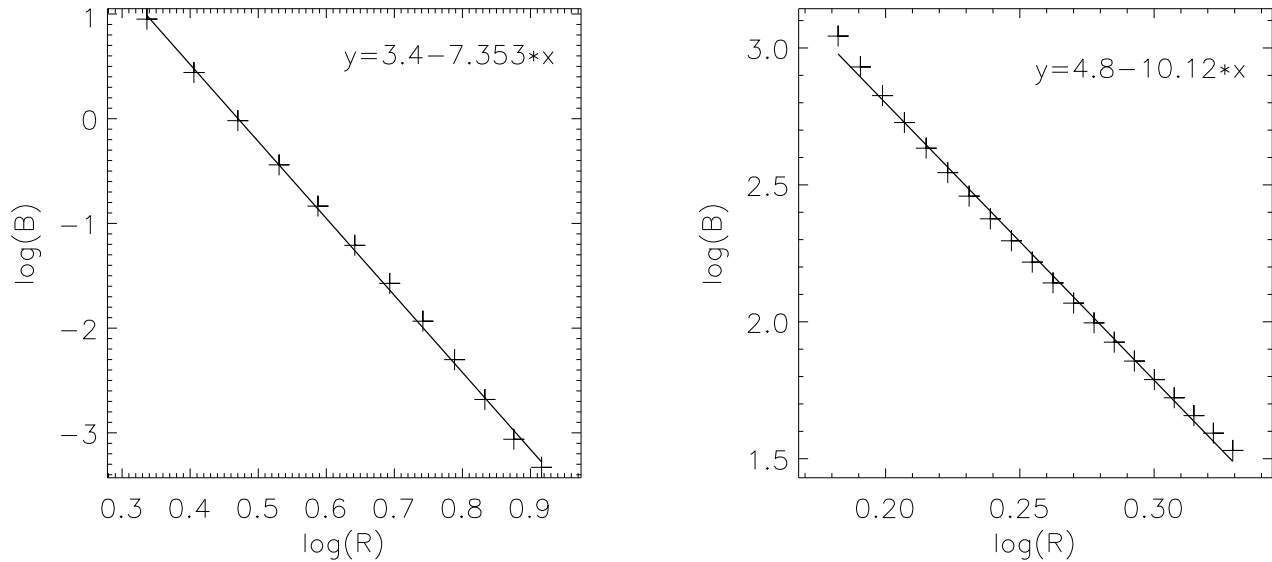


Fig. 1.— An example of fittings of magnetic field strength and height for the 2000 June 6 event. The strength and height are in logarithm. The symbol of ‘+’ represents calculated data while the solid lines are results of a linear fitting to the data. The slope here is actually the decaying index detailed in the text. Shown in the left panel is the fitting for the data from 1.4 Rs to 2.5 Rs. The right panel shows a fitting for the low altitude data (from 1.1 Rs to 1.3 Rs). Here Rs denotes solar radius.

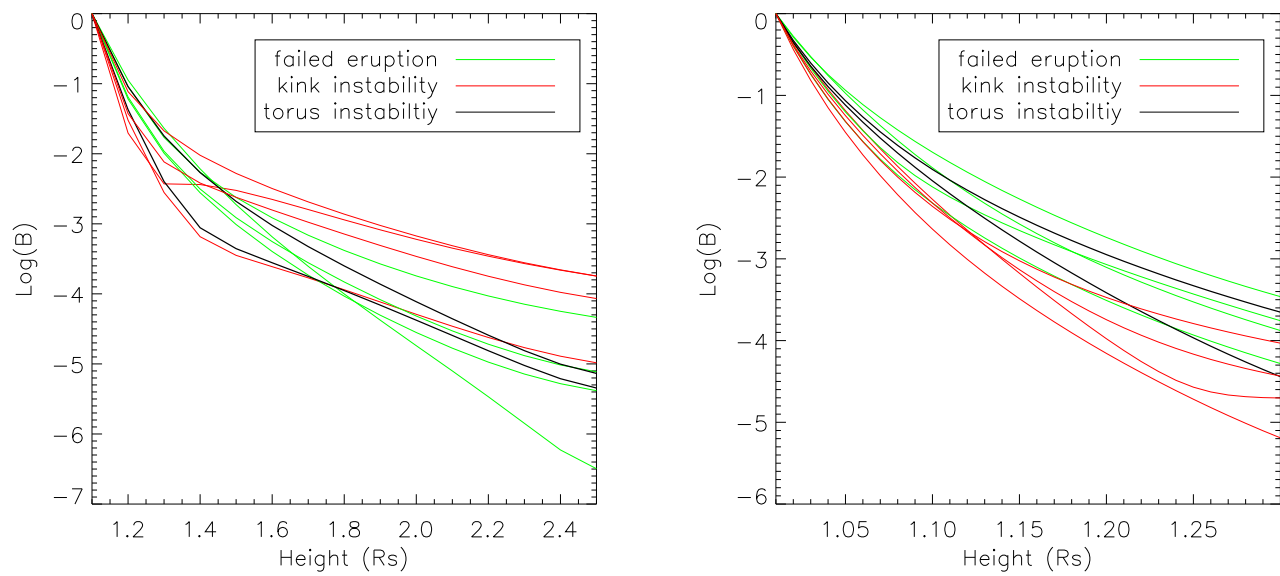


Fig. 2.— Profile of magnetic field above the erupted filaments. The field strength is in logarithm. Left: from 1.1 Rs to 2.5 Rs. Right: from 1.01 Rs to 1.20 Rs.

Table 1: List of the events in this study

Type ^a	Flare	Date, Time ^b (dd/mm/yy, UT)	Active Region NOAA	n ₁ ^c	n ₂ ^d	B ^e (Gauss)	Source ^f
TI	M4.0	16/06/05 1910	0775	3.97	15.2	9.55	S
TI	M3.7	27/07/05 0300	0792	4.95	10.8	10.0	S
KI	C6.8	07/04/97 1350	8027	2.95	10.0	4.53	G
KI	C1.3	12/05/97 0442	8038	2.89	13.0	5.84	G
KI	M6.3	15/06/01 0952	9502	2.38	16.1	12.9	G
KI	X2.5	10/11/04 0156	0696	3.12	15.9	14.3	W
FE	X1.1	06/06/00 1330	9026	7.35	10.1	23.7	G
FE		19/07/00 2330	9077	4.52	12.1	17.4	G
FE		27/05/02 1805	9957	3.52	11.1	23.1	G
FE	M1.0	02/05/03 0247	0345	4.88	12.3	44.3	G

^aTypes of eruption. *TI* represents torus instability eruption. *KI* means kink instability eruption. *FE* denotes failed eruption of kink instability.

^bDate and time of the occurrence of flares.

^cDecaying index (see text for more detail) derived from the data from 1.4 Rs to 2.5 Rs. Rs denotes solar radius.

^dDecaying index derived from the data from 1.1 Rs to 1.3 Rs.

^eAverage magnetic strength at 1.1 Rs. The field is averaged over the active region

^fThe source of the events. *S* denotes the events from Schrijver et al. (2007). *G* denotes the events from Green et al. (2007). *W* denotes event from Williams et al. (2005)

Table 2: Three types of eruption: average

Type	n ₁ (1.4Rs-2.5Rs)	n ₂ (1.1Rs-1.3Rs)	B (at 1.1Rs)
TI	4.46 ± 0.49	13.0 ± 2.2	9.77 ± 0.22
KI	2.83 ± 0.22	13.7 ± 2.2	9.39 ± 4.20
FE	5.06 ± 1.14	11.4 ± 0.8	27.1 ± 8.5
KI+TI	3.37 ± 0.72	13.5 ± 2.2	9.52 ± 2.89